Larhyss Journal, ISSN 1112-3680, n°53, Mars 2023, pp. 165-182

INVESTIGATION OF HISTORICAL EXTREME RAINFALL ON PERMEABLE ROAD IN A COMMERCIAL CENTRE

MAH D.Y.S.[1,*], DAYANG NUR HUWAIDA A.S.[2], TEO F.Y.[3]

[1] Associate Professor, UNIMAS Water Centre, Faculty of Engineering, Universiti Malaysia Sarawak, 94300 Kota Samarahan, Sarawak, Malaysia
[2] Graduate Research Assistant, Faculty of Engineering, Universiti Malaysia Sarawak, 94300 Kota Samarahan, Sarawak, Malaysia
[3] Associate Professor, Faculty of Science and Engineering, University of Nottingham Malaysia, 43500 Semenyih, Selangor, Malaysia

(*) ysmah@unimas.my

Research Article – Available at http://larhyss.net/ojs/index.php/larhyss/index
Received January 6, 2023, Received in revised form March 11, 2023, Accepted March 12, 2023

ABSTRACT

Urban development areas, having greater impervious surfaces such as roads, parking spaces and building roofs, have an adverse impact on the urban environment, as they generate more runoff. This situation could even worsen during extreme rainfall events as it accumulates stormwater runoff more rapidly and causes the occurrence of flash floods. In this study, eight historical extreme rainfall events with rainfall depths between 40 and 70 mm were chosen to investigate the performance of permeable pavement as an urban runoff mitigation measure approach in stormwater management. A commercial center was selected as a case study, with a total catchment area of 3,425 m^2 and consisting of double-row roadside car parking spaces with tarred surfaces covering 61% of the total catchment area. The front road of the shophouses was assumed to be replaced with a modular-based precast stormwater detention system, and a drainage model was developed to mimic the system. Simulations of the stormwater flowing through the detention system were performed with Storm Water Management Model version 5.0, and it was found that the detention system could endure seven out of the eight storms. The only storm that overwhelmed the system demonstrated an intense rainfall pattern that peaked in the first hour.

Keywords: Drainage, Hydrograph, Urban runoff, Permeable road, Postdevelopment, Predevelopment, Sustainable development.

INTRODUCTION

The practice of evaluating water infrastructures such as irrigation and drainage systems against historical extreme rainfall events is common. It is based on the understanding that if a structure could withstand the intensities and amounts of rainwater from extreme events, it has a high capability as a flood mitigation structure. This is in agreement with the study of Notaro et al. (2015), who reported that changes in the intensities of extreme rainfall impacted urban drainage systems. As such, this study applies selected extreme rainfall events to investigate the effectiveness of permeable pavement.

In addition, Ziang et al. (2019) described a study that used artificial rainfall simulation experiments to analyze the permeable pavement area proportion effect on the overall structure of rainwater regulation ability, in which the study found that the porous structure of permeable pavement had great performance in terms of the adsorption capacity and permeability of rainfall runoff.

Generally, permeable pavement is an engineering structure with a significant layer of porous materials that contain more air voids than conventional impermeable pavement (Li et al., 2013). The porous layer allows stormwater to permeate through and another significant layer with storage underneath the aforementioned porous layer to hold the permeated water. This study focuses on precast-concrete permeable pavement, and four examples of such a type of precast-concrete structure are presented in Figure 1.

Precast concrete is a strong construction material that can be molded into different forms (Kia et al., 2021). Concrete panels (Fig. 1a), arcs (Fig. 1b), rectangular boxes (Fig. 1c) and modular units (Fig. 1d) provide flat surfaces that could be applied as low-volume roads or car parking lots. Usually, service inlets could be installed on the concrete frames to drain rainwater and hence provide a function of porosity to the precast concrete structures. Bounded by the concrete frames, empty chambers are created inside the precast concrete pieces to hold water (Guan et al., 2021).

The type of precast concrete pavement chosen for study is a noncommercialized research product named the StormPav Green Pavement System or, in short, StormPav. Developed by Universiti Malaysia Sarawak and collaborators, StormPav uses a Grade 50 concrete mix in the casting process to cater to a crushing load up to 100 kN/unit (Mah et al., 2022). In this study, StormPav modular units are assumed to replace a stretch of tarred surfaces in front of shophouses (Fig. 2), which is further described in the Materials and Methods.

StormPav consists of three precast concrete pieces that form a single modular unit, namely, a top cover, a cylinder and a bottom plate. The 0.1624 m^2 cover is equipped with a 0.04 m diameter service inlet to drain water. The 0.03 m high hollow cylinder with an inner diameter of 0.28 m and a wall thickness of 0.06 m receives the drained water and acts as a storage chamber. Recent studies have noted that another function of conveying permeated water, such as in road drainage, is possible. As stated by Mah et al. (2020), a permeable road system could be an alternative to the existing road drainage system to simultaneously hold and flow rainwater below the road.

Figure 1: Precast-concrete permeable pavements in the forms of a) panel (https://oldcastleinfrastructure.com), b) arc (https://www.kistner.com/), c) box (https://precast.org/) and d) modular unit (https://stormtrap.com)

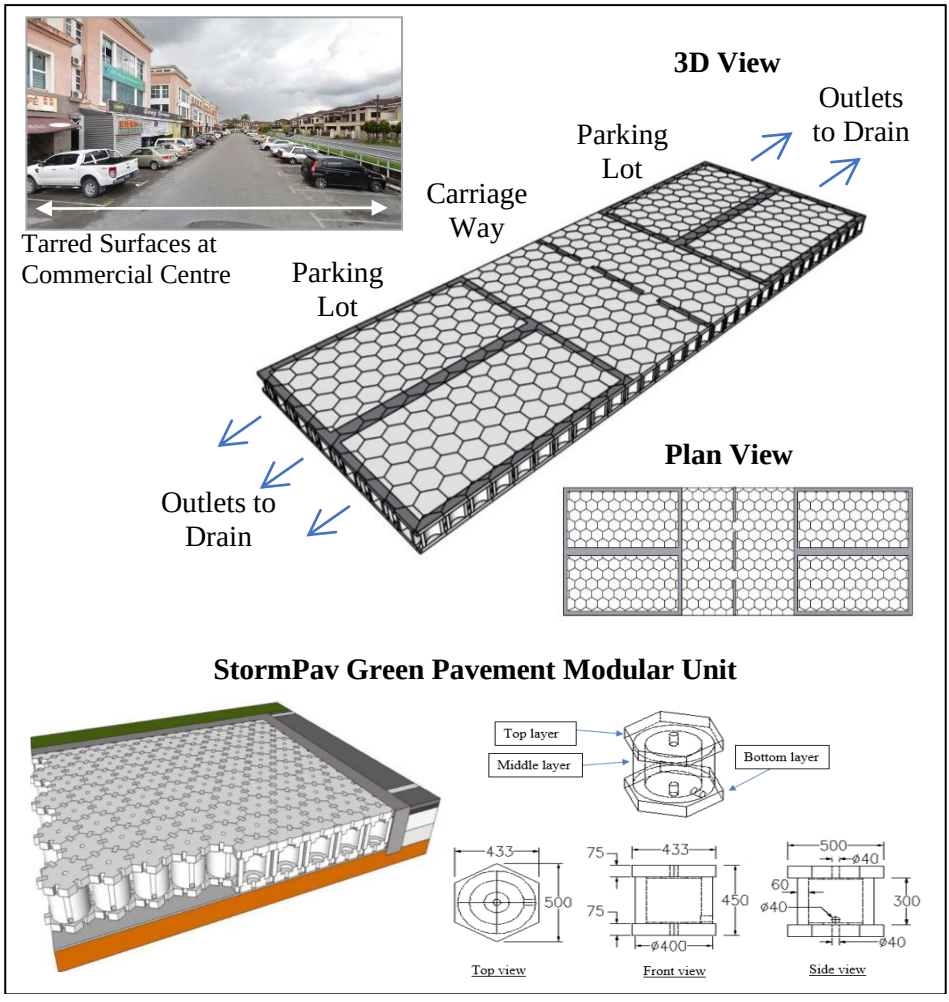

Figure 2: Application of StormPav Green Pavement as a permeable road in a commercial center

THEORY

In line with the latest development of permeable pavement, this study explored the stormwater detention characteristics of StormPav modular units when subjected to extreme rainfall. Generally, the tarred surface areas of any commercial center are high due to the car parking lots to accommodate vehicles. This situation leads to increasing impervious surfaces that restrict infiltration and increase the amount of surface runoff (Rathnayke and Srishantha, 2017).

Theoretically, the combined multiple StormPav modular units function as a detention tank, in which the amount of surface runoff generated on the tarred surfaces is directed to the subsurface detention system. The rate of water permeated from the tarred surfaces to the system is defined as the volume of water entering over time and is termed the detention inflow (Q_{in}). The water is released via an outlet, usually in the form of an orifice, which regulates the volume of water leaving over time and is termed the detention outflow (Q_{out}). The mentioned inflow and outflow hydrographs are presented in Fig. 3. The graph area bounded by the two hydrographs is the volume of water being detained (V_s).

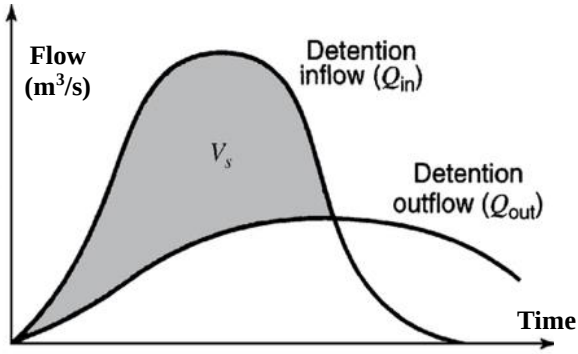

Figure 3: Characterization of stormwater detention

MATERIAL AND METHODS

The study began with the collection of extreme rainfall data based on past flood events. With a selected commercial center, the catchment characteristics and dimensions of the existing structures in the study area, such as roads and drains, were measured. The associated drainage system in the commercial center was simulated using the Storm Water Management Model (SWMM) version 5.0. Inflow and outflow data generated by the model due to the selected extreme rainfall events were evaluated.

Extreme rainfall events

For Kuching and Samarahan in the southern region of Sarawak, Malaysia, the designed rainfall for a minor drainage system in a small catchment area (0.2 - 2 ha) subjected to a 5-minute and 10-year average recurrent interval (ARI) was estimated as 23 mm (PUB, 2010; DID, 2012). On the other hand, extreme rainfall can be described as the amount of rainfall received exceeding the design rainfall for a given period.

It is common for rainfall events to become severe when coinciding with the monsoon season, in the case of Sarawak, the northeast monsoon season. This monsoon season occurs between November and February and is usually associated with heavier rainfall. Eight (8) storm events with peak rainfall readings exceeding 30 mm were selected from 2015 to 2021 and occurred in the months of December, January and February (Table 1). These storms were reported with subsequent flooding in Kuching and Samarahan.

Table 1: Selected storms that occurred in the Kuching and Samarahan areas (Sourced from Department of Irrigation and Drainage Sarawak)

No	Date	Peak Rainfall Depth (mm)	Duration of Storm (Hour)	Total Rainfall (mm)
Event 1	18 & 19 January 2015	38.5	11	107.5
Event 2	19 January 2015	43	14	188.0
Event 3	1 January 2016	51	6	89.5
Event 4	17 & 18 December 2017	47.5	15	178.5
Event 5	11 & 12 December 2019	70.5	15	131.0
Event 6	16 January 2020	41.6	4	52.6
Event 7	22 February 2020	47.6	10	117.5
Event 8	13 & 14 January 2021	69.5	7	193.0

Study area

A commercial center called Palm Square was chosen as the case study (Figure 4). Its location is beside Dato' Mohd Musa Road, a major road connecting Kuching and Samarahan. The commercial center has one row of shophouses. Tarred roads and parking spaces are found surrounding the shophouses. It also has two different sizes of the concrete drain, which are 0.5 m x 0.5 m and 1 m x 1 m.

The total area of the catchment is 3,425 m^2 (0.3 ha). Approximately 39% of the catchment, which is 1332 m^2, is occupied by the shophouses that consist of 10 units of double-storey shophouses. There are two corner shophouses with a measurement of 18 m x 9 m each and eight intermediate shophouses with a measurement of 18 m x 7 m each. The remaining 61% of the catchment, which is 2093 m^2, is covered by tarred roads and parking spaces. The front road has 5 m wide parking lots on two sides of the road and a 4 m wide carriageway in between. The back lane has a row of motorcycle parking lots and a 4 m wide carriageway. To accommodate the study of permeable roads, the stretch of 74 m

long and 14 m wide tarred surface in front of the shophouses was assumed to be replaced with StormPav. Its outlets are in the form of 0.05 m diameter round orifices.

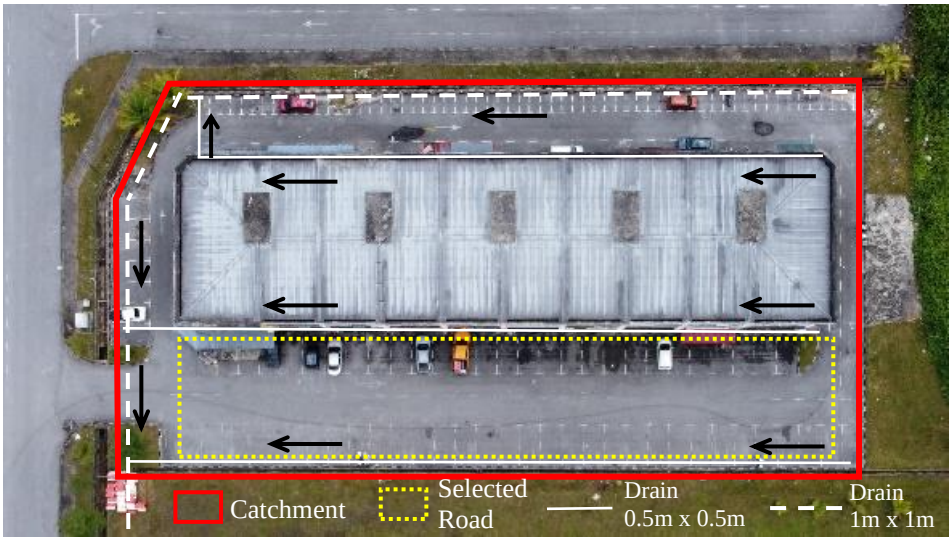

Figure 4: Study area

Modeling approach

The simulation of stormwater runoff through catchments and drainage systems was conducted using the Storm Water Management Model (SWMM) version 5.0. Simulation software is capable of computing stormwater runoff data to provide a solution for reducing runoff volume in urban areas (Lisenbee et al., 2022). The developed SWMM model for the study area is presented in Figure 5.

The modeling steps start by inserting the historical extreme rainfall data onto the model via its "Rainfall" interface, which generates runoff onto the connected "Catchment". Roofs, roads and parking lots represent the "catchments". From "catchments", running water is directed to either permeable roads or drains. "Storage Units" and "Orifices" represent the StormPav permeable road, in which the tarred surfaces are divided into half following the road crown and allowing the running water to flow along the slope of the road crown. "Nodes" and "Links" represent the series of concrete drains. The running water from the whole system eventually leaves at the "Outfall" (Hamouz and Muthanna, 2019). A flow chart of the modeling approach is presented in Figure 6.

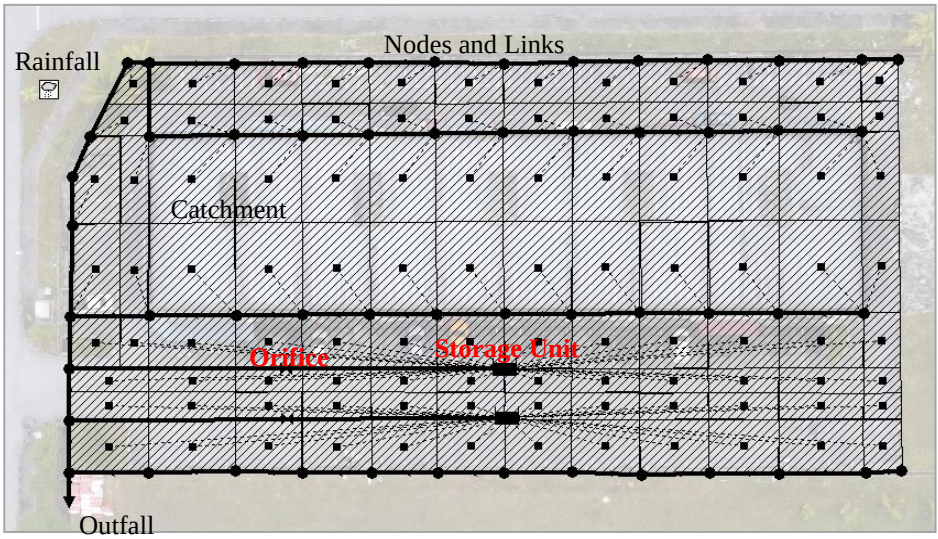

Figure 5: Developed SWMM model

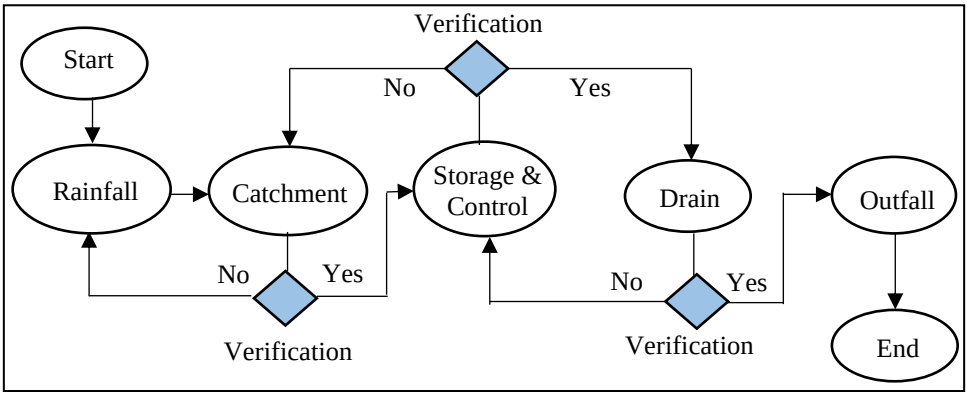

Figure 6: Flow chart for modeling approach

SWMM applies a nonlinear differential equation of sheet flow to generate runoff:

$$Q_a = W\frac{1.49}{n}\left(d - d_p\right)^{5/3} S_c^{1/2} \quad (1)$$

where Q_a = catchment flow (m^3/s); W = width of catchment (m); Sc = slope of catchment (m); n = Manning roughness value ($s/m^{1/3}$); d_p = maximum depression storage (m); and d= depth of water over the catchment (m).

Once the catchment flow was directed to a node, SWMM routes the running water from node to node through the channel using kinematic wave approximation:

$$Q_b = \frac{\partial A}{\partial t} + \alpha m A^{m-1} \frac{\partial A}{\partial x} \quad (2)$$

where Q_b = Routed drain flow (m^3/s); A = Cross-sectional area of the drain (m^2); x = Distance along the flow path (m); t = Time step (s); α = Flow geometry due to drain (unitless); and m = Surface roughness of drain (unitless).

A stormwater detention structure in SWMM is represented as the water balance because of running water flowing in and out of the structure:

$$S_t = \sum_i (Q_i - Q_0)\, \Delta t_s \quad (3)$$

where St = Storage volume (m^3); Q_i = Inflow (m^3/s); Q_o = Outflow (m^3/s); and t_s = Duration of storm (s).

The catchment, storage and drain are the chosen model components as control parameters to verify the implemented model. To verify the SWMM computed values, other formulas are used to check the model. Generally, catchment flow can be estimated using a rational method:

$$Q_c = \frac{CIA_D}{360} \quad (4)$$

where Q_c = catchment flow (m^3/s); C = runoff coefficient (unitless); I = rainfall intensity (mm/hr); and A_D = drainage area (ha).

The design of the usually concrete drain could be referred to the Manning formula:

$$Q_d = \frac{1}{n} A_f R^{2/3} \sqrt{S_f} \quad (5)$$

where

Q_d = Drain flow (m^3/s); n = Manning's roughness coefficient ($s/m^{1/3}$); A_f = Flow area of drain (m^2); R = Hydraulic radius of drain (m); and S_f = Friction slope of drain (m/m).

For the catchment, a scatter plot of modeled and theoretical flow data is presented in Figure 7a. The plot compares values generated from Equations 1 and 4, which give an R-squared value of 0.89.

For storage, a comparison of the modeled and theoretical storage inflows is presented in Figure 7b. Running water permeates through the road catchments and flows to the storage is considered the inflow to the storage. The theoretical storage inflow can be calculated using Equation 4 and compared with Equation 1 for catchments connected to the detention storage only. The R-squared value for the storage flow is 0.89.

For the drain, the scatter plot of modeled and theoretical drain flows presents an R-squared value of 0.89. SWMM utilizes the kinematic wave approximation for flow routing as in Equation 2. The theoretical drain flow is calculated using the Manning formula in Eq. 5.

The three components obtain R-squared values greater than 0.6, which indicates that the verification is acceptable. The R-squared value outlines the degree of collinearity between the simulated and measured data. According to Pereira Souza et al. (2019) and Zakizadeh et al. (2022), the R-squared value should be at least 0.6 to reach a satisfactory rate of model performance.

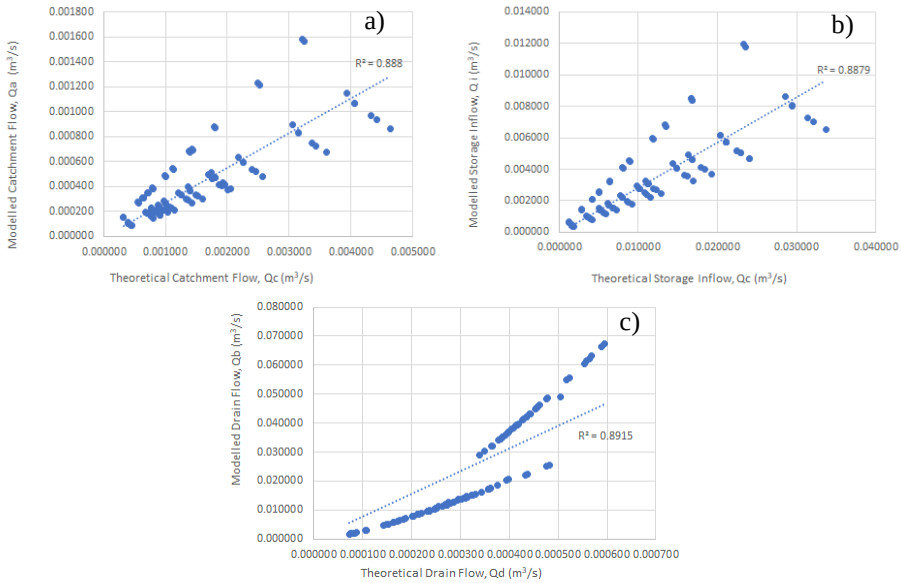

Figure 7: Model verification of modeled and theoretical flows, a) catchment flow, b) inflow to storage and c) drain flow

RESULTS AND DISCUSSION

Stormwater Detention Characteristics

The StormPav road was modeled with two storage units (refer to Figure 5) serving the selected road catchment (74 m x 14 m). Due to the symmetrical nature of dividing the road into two catchments (74 m x 7 m each), choosing either of the storage units is expected to give similar results. The stormwater detention characteristics herein refer to one of the storage units regulated by a 0.05 m diameter orifice at the bottom of the tank, with an estimated storage capacity of 98.4 m^3.

Half of the StormPav road is expected to be assembled with 3190 modular units, each with a 0.04 m diameter service inlet. These service inlets serve as the inlet to the subsurface detention. On the other hand, only one outlet for one storage unit is allowed in the simulation. Generally, the subsurface detention functions like a water draining tank,

in which water is allowed to flow in and out at the same time. The outlet is the main control of water draining; when the outlet is too large, water is released in a free-flowing manner; when the outlet is too small, water cannot be released in time, causing the accumulation of water volumes in the tank to increase and possibly overtop the tank.

Simulated inflow and outflow hydrographs of the selected storage unit due to the eight selected extreme rainfall events are presented in Figure 8. Rainfall hyetographs of the eight storms are inserted in the same figure as well. Generally, the patterns of the rise and fall of the hydrographs follow the theoretical inflow and outflow hydrographs depicted in Figure 3. The inflow hydrographs are found to fluctuate following the intensities of the storm, while the outflow hydrographs are more stable due to the fixed orifice outlet. The flow through the orifice outlet is full-pipe flow over the course of storms.

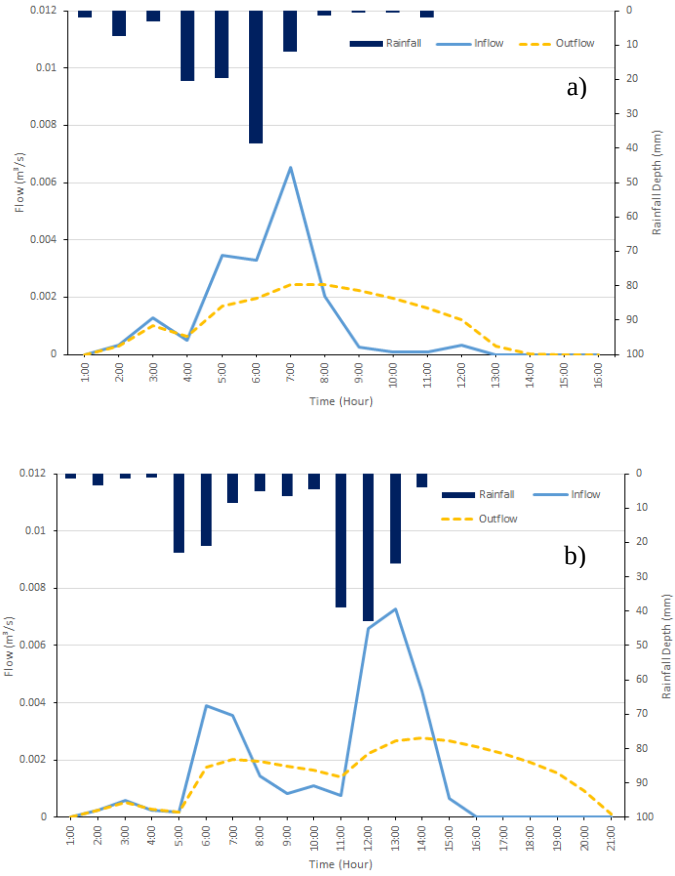

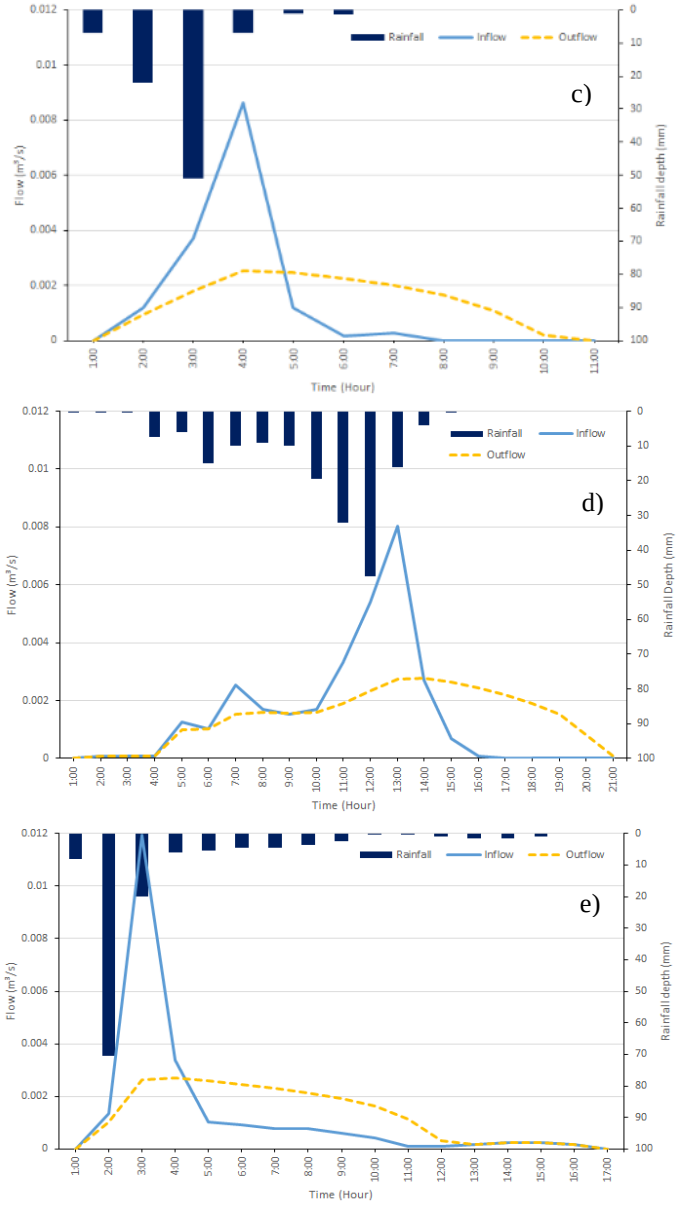
c)
Rainfall
Inflow
Outflow
Flow (m³/s)
Rainfall depth (mm)
Time (Hour)
d)
Rainfall
Inflow
Outflow
Flow (m³/s)
Rainfall Depth (mm)
Time (Hour)
e)
Rainfall
Inflow
Outflow
Flow (m³/s)
Rainfall depth (mm)
Time (Hour)

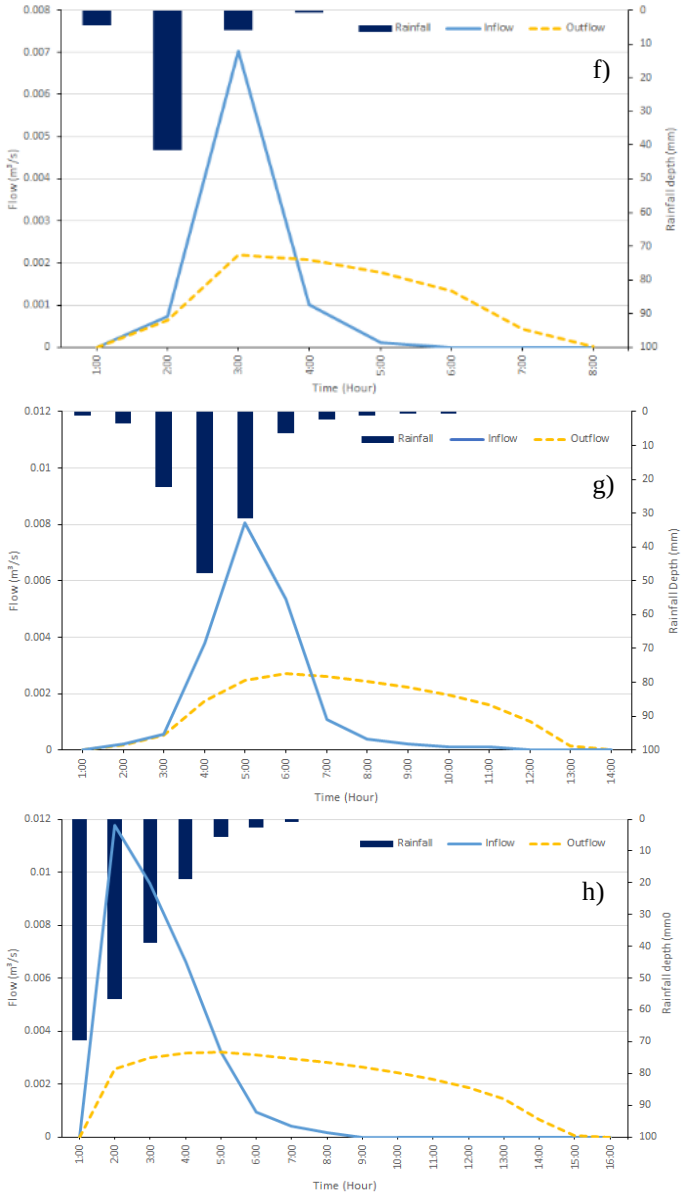

Figure 8: Hydrographs of detention inflow and outflow subjected to a) 18 and 19 January 2015, b) 19 January 2015, c) 1 January 2016, d) 17 and 18 December 2017, e) 11 and 12 December 2019, f) 16 January 2020, g) 22 February 2020 and h) 13 and 14 January 2021

DISCUSSION

Data from the stormwater detention characteristics are extracted and plotted against captured water levels in the storage layer (Figure 9). The maximum height of the layer of hollow cylinders that functions as the water storage chamber is 0.3 m, and red lines are added in the figure to indicate this maximum water level. Any water levels modeled above 0.3 m would indicate failure of the detention system with overflowing stormwater.

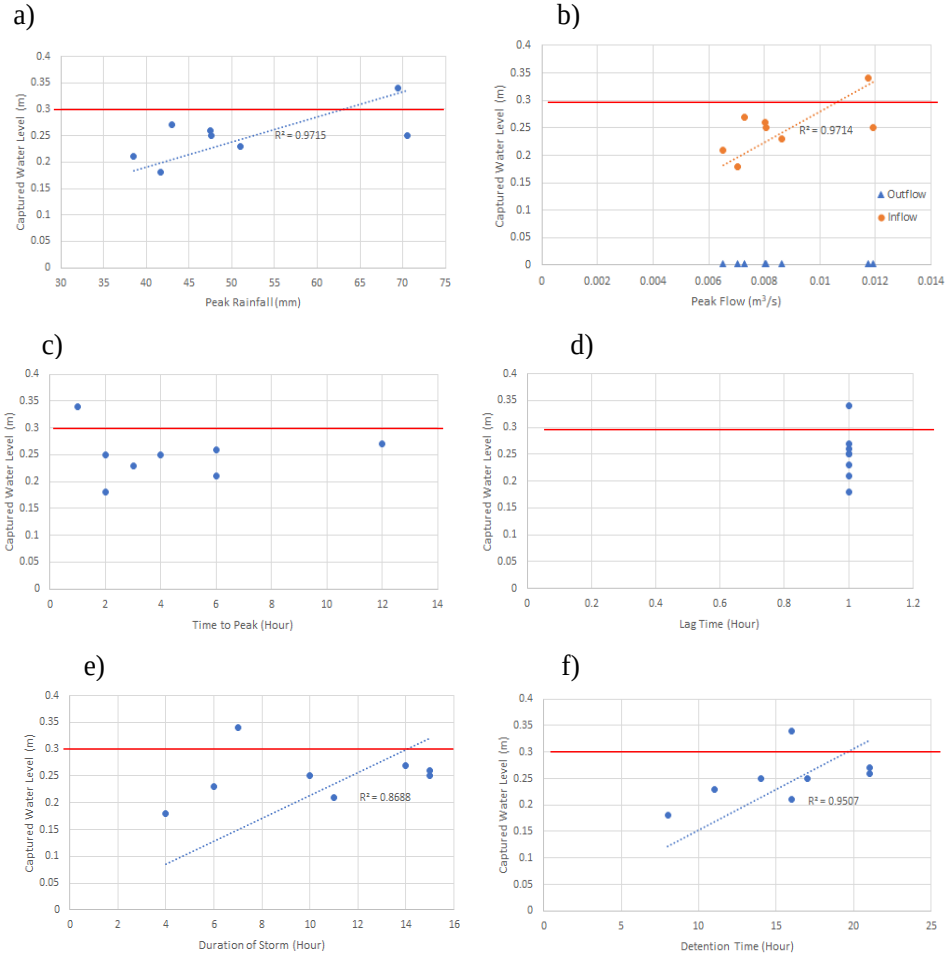

Figure 9: Relationships of captured water levels in the detention system due to the eight selected storms in terms of a) peak rainfall, b) peak inflow and outflow, c) time to peak, d) lag time, e) duration of storm and f) detention time (red lines indicate maximum height of the storage layer)

Relationship with peak rainfall

The plot of water level against peak rainfall is presented in Figure 9a. Seven storms had maximum water levels below 0.3 m, while one storm (Event 8) had maximum water levels above 0.3 m. Six storms had peak rainfall between 40 and 50 mm, and the data show that higher peak rainfall did not warrant higher water levels. Although the remaining two events had similar 70 mm peak rainfall, one event (Event 8) had a water level above 0.3 m, and another had a water level below 0.3 m. Event 8 repeatedly appeared in other subfigures with distinctive characteristics that differed from those of the other seven storms.

Relationships with peak inflow and outflow

The plot of water level against inflow and outflow is presented in Figure 9b. The inflows from the eight storms fluctuated, in which six storms had peak inflow data between 0.006 and 0.009 m^3/s. These inflows produced water levels below 0.3 m. The same trend in the remaining two storms is repeated, similar to the trend in the previous subsection. Although the two storms produced the highest inflow data, namely, 0.012 m^3/s, one (Event 8) produced a water level above 0.3 m and another below 0.3 m.

In contrast with the inflow data, the outflow data are identical throughout the eight events. This is due to the orifice outlet control, which regulated the water leaving the detention system. The outlet managed seven out of the eight storms without overflowing, except Event 8.

Relationships with time to peak and lag time

The plot of water level against time to peak is presented in Fig. 9c. Six storms had times to peak between 2 and 6 hours, and one storm had 12 hours. These seven storms did not cause overflowing in the subsurface detention system. The only storm (Event 8) that exceeded the maximum water level had a time to peak in the first hour. This suggests that a time to peak of at least two hours shall give the flow mechanism in the detention system adequate time to receive and release water at the same time.

The plot of water level against lag time is presented in Fig. 9d. All the storms had a lag time of one hour. However, only one storm produced a water level above 0.3 m, while the rest of the storms were not. Therefore, the lag time had little influence on the detention system.

Relationships with storm duration and detention time

The plots of water level against storm duration and detention time are presented in Figures 9e and 9f, respectively. The storm durations were in the range of 2 to 15 hours. Event 8, which had a storm duration of 7 hours, was observed to cause overflowing in the detention system. No clear relationship could be deciphered from the graph.

The detention times were in the range of 8 to 21 hours. Similarly, Event 8 was the only storm that had caused overflowing and had a detention time of 16 hours. No clear relationship could be deciphered from the graph.

Limitations

The detention system was modeled to receive water from the road surfaces above the subsurface detention. It excluded any additional surface runoff from nearby catchments.

Water storage structures are equipped with overflow outlets. However, the overflow outlet was excluded in the modeling effort. SWMM can only model one outlet for a storage unit at a time. Therefore, the orifice outlet was prioritized over the overflow outlet.

CONCLUSION

A stretch of road in a commercial center was assumed to be replaced with StormPav modular units. These modular units, once assembled, would function like a water draining tank with an orifice outlet. With a case study with known catchment measurements and the StormPav modular unit with known related flow characteristics, the mentioned system was modeled in SWMM version 5.0. Eight selected extreme rainfall events were run through the model.

The modeling results indicated that the detention system was able to contain seven out of the eight storms. The remaining storm, which caused overflowing, suggested that the storm peaked in the first hour as the main reason for flooding. However, the conclusion is preliminary, as it came from one storm. Further study should be carried out to explore more storms peaking at the first hour of various intensities and time stamps of storm burst in the performance of stormwater detention systems.

Declaration of competing interest

The authors declare that they have no known competing financial interests or personal relationships that could have appeared to influence the work reported in this paper.

ACKNOWLEDGEMENT

The authors acknowledge financial support from the International Matching Grant Scheme between Universiti Malaysia Sarawak and Universitas Pembangunan Jaya under the research program entitled “Flood Infrastructure for Sustainable Urban Development”.

REFERENCES

DEPARTMENT OF IRRIGATION AND DRAINAGE (DID) OF MALAYSIA (2012). Urban Stormwater Management Manual for Malaysia, Ministry of Environment and Water, Kuala Lumpur.

GUAN X., Wang J., Xiao F. (2021). Sponge City Strategy and Application of Pavement Materials in Sponge City, Journal of Cleaner Production, Vol 303, 127022.

HAMOUZ V., MUTHANNA T.M. (2019). Hydrological Modelling of Green and Grey Roofs in Cold Climate with the SWMM Model, Journal of Environmental Management, Vol. 249, 109350.

KIA A., DELENS J.M., WONG H.S., CHEESEMAN C.R. (2021). Structural and Hydrological Design of Permeable Concrete Pavements, Case Studies in Construction Materials, Vol. 15, e00564.

LI H., HARVEY J.T., HOLLAND T.J., KAYHANIAN M. (2013). The Use of Reflective and Permeable Pavements as a Potential Practice for Heat Island Mitigation and Stormwater Management, Environmental Research Letters, Vol 8, No 1, 015023.

LISENBEE W.A., HATHAWAY J.M., WINSTON R.J. (2022). Modelling Bioretention Hydrology: Quantifying the Performance of DRAINMOD-Urban and the SWMM LID Module, Journal of Hydrology, Vol. 612, 128179.

MAH D.Y.S., BUSTAMI R.A., PUTUHENA F.J., AL DIANTY M. (2020). Testing the Concept of Mitigating Overflowing Urban Drain with Permeable Road, International Journal of Advanced Trends in Computer Science and Engineering, Vol. 9, No 5, 7878-7882.

MAH D.Y.S., NGU J.O.K., TAIB S.N.L., LIM S.F., PUTUHENA F.J. (2022). Testing the Concept of Mitigating Urban Flooding with Permeable Road: Case Study of Tong Wei Tah Street, Kuching, Sarawak, Malaysia, Trends in Sciences, Vol. 19, No 15, 5592.

NOTARO V., LIUZZO L., FRENI G., LA LOGGIA G. (2015). Uncertainty Analysis in the Evaluation of Extreme Rainfall Trends and its Implications on Urban Drainage System Design, Water, Vol. 7, No 12, 6931-6945.

PEREIRA SOUZA F., LEITE COSTA M.E., KOIDE S. (2019). Hydrological Modelling and Evaluation of Detention Ponds to Improve Urban Drainage System and Water Quality, Water, Vol. 11, No 8, 1547.

PUBLIC UTILITIES BOARD (PUB) OF SINGAPORE (2010). Technical Guide for On-Site Detention Tank Systems, National Water Agency, Singapore.

RATHNAYKE U., SRISHANTHA U. (2017). Sustainable Urban Drainage Systems (SUDS) – What It Is and Where Do We Stand Today?, Engineering and Applied Science Research, Vol. 44, Issue 4, pp. 235-241.

ZAKIZADEH F., MOGHADDAM NIA A., SALAJEGHEH A., SAÑUDO-FONTANEDA L.A., ALAMDARI N. (2022). Efficient Urban Runoff Quantity and Quality Modelling Using SWMM Model and Field Data in an Urban Watershed of Tehran Metropolis, Sustainability, Vol. 14, No 3, P. 1086.

ZIANG Z., XIE J., GU S., GAO L., LIU, Y. (2019). Study on Hydrological Characteristics of Large Permeable Parking lot in Sponge City, IOP Conference Series: Earth and Environmental Science, Vol. 295, No 3, 032019.